Turkish Online Journal of Qualitative Inquiry (TOJQI)
Volume 12, Issue 6, June 2021: 963- 970

Computational Analysis of Performance of a Transonic Fan Blade

Shravan Kumar S[a], Nagireddy Mallikarjunareddy[b], B Talpa Sai Prasad[c]

[a,b,c]School of Aeronautical Sciences, Hindustan Institute of Technology and Science, Padur, Chennai

[a] shravank0510@gmail.com

Abstract

This paper aims to study the performance of the NASA Rotor 67 transonic fan blade at various operating conditions. First, a steady-state computation along with mesh independence study is done using ANSYS CFX at the design operating speed of the rotor. Then the analysis is carried out at 86%, 92%, 96%, and 105% of the design operating speed. The performance of the rotor is compared and analysed for various off-design operating conditions to evaluate the flow behaviour in transonic speed through the highly twisted fan rotor blade.

Keywords: off-design, flow behaviour, operating speed, transonic flow, NASA Rotor 67.

1. Introduction

Nasa Rotor 67 is a popular validation test case for turbomachinery. It is an axial compressor Rotor consisting of 22 blades. A detailed study of the rotor was conducted by Strazisar et al. using a laser anemometer experiment to study the properties of the rotor [1]. A brief list of specifications is given in Table 1. [1][2][3]

Number of Blades	22
Designed Mass Flow Rate	33.25 kg/s
Designed Rotational Velocity	16043 rpm
Tip Speed	429 m/s
Hub-Tip ratio at inlet/outlet	0.375/0.478
Rotor Aspect Ratio	1.56
Design Pressure Ratio	1.63
Span	130 mm
Mid-Span Chord Length	95 mm
Design Tip Inlet Mach No	1.37

Table 1: Nasa Rotor 67 Design Specifications

In this paper, the speed of the rotor was varied to obtain the various performance curves at those speeds. The analysis of the curves will give us a clue to how the rotor performs at off-design speeds.

2. Steady State Analysis and Grid Independence Study

2.1 Pre-Processing for Steady State Analysis

Using a model of the Rotor, a tetrahedral mesh was generated using Ansys Mechanical Mesh.The mesh (Fig 1) consisted of around 443k nodes and 368k elements.

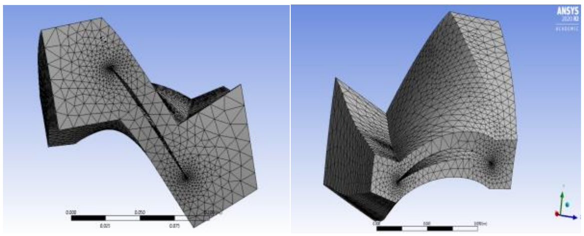

Figure 1 Mesh Generated for Steady State Analysis

The pre-processing was done using ANSYS CFX. The inlet boundary conditions (Table 2) are similar to the boundary conditions for a clean inlet specified in [2].

Fluid Definition	Air Ideal Gas
Rotational Speed	16043
Inlet Relative Pressure	1atm
Inlet Temperature	288K
Outlet Gauge Pressure	0Pa
Convergence Control	Max Iterations: 1500
Advection Scheme	Upwind
Convergence Criteria	Residual Target 1e-6
Turbulence Modelling	Shear Stress Transport

Table 2: Inlet Boundary Conditions

The CEL expressions given below was added to calculate the pressure ratio of the rotor.

massFlowAve(Total Pressure in Stn Frame)@ R1 Outlet/ massFlowAve(Total Pressure in Stn Frame)@ R1 Inlet [4]

2.2 Pre-Processing for Grid Independence Study

A grid independence study was done to check the influence of the grid on the results. Four different meshes were developed for the four cases mentioned in Table 3. The boundary conditions used for this analysis is the same as the one mentioned in Table 3. The results of the grid independence study are discussed in Section 2.3

	Case 1 (-15%)	Case 2 (-10%)	Case 3 (+10%)	Case 4 (+15%)
Number of Nodes	378888	398204	486372	507610
Number of Elements	271200	285285	348831	364421

Table 3 Mesh Details of Grid Independence Study

2.3 Results for Steady State and Grid Independence Study

Figures 3 shows the Mach Number Distribution Contours obtained from the steady state analysis. The pressure ratio obtained was 1.65, which is very close to the design pressure ratio of 1.63. The contours show that a shock is formed at around 70% of the chord at the pressure surface and near the leading edge on the pressure surface as predicted by Doi et al. [5]. Fig 2 shows the Coefficient of Pressure Distribution at 50% of the span

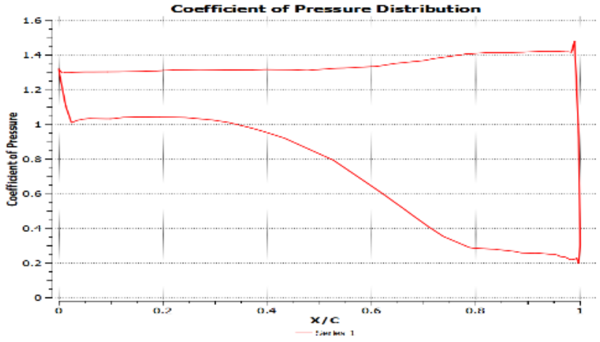

Fig 2 Coefficient of Pressure Distribution

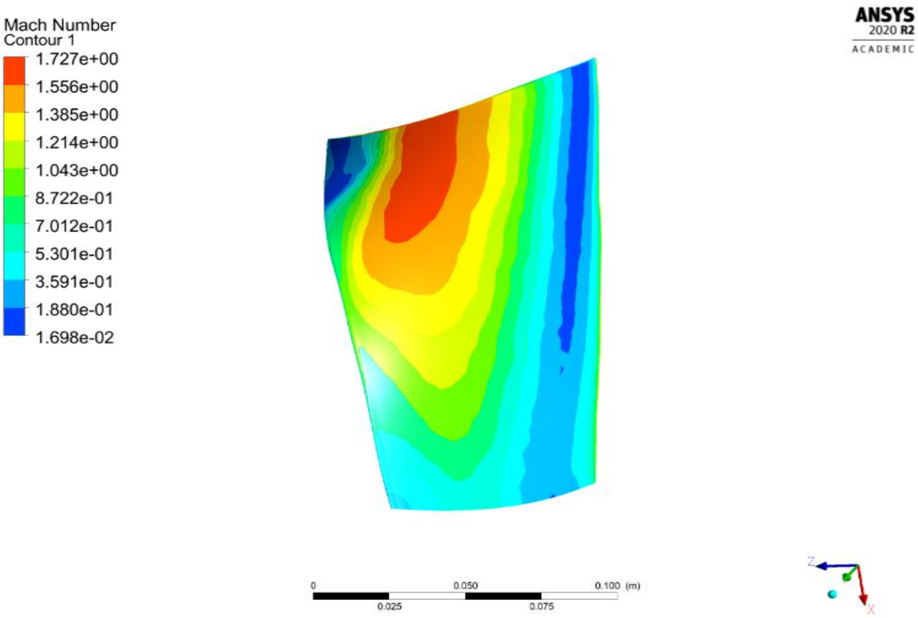

Figure 3 (a) Pressure Surface

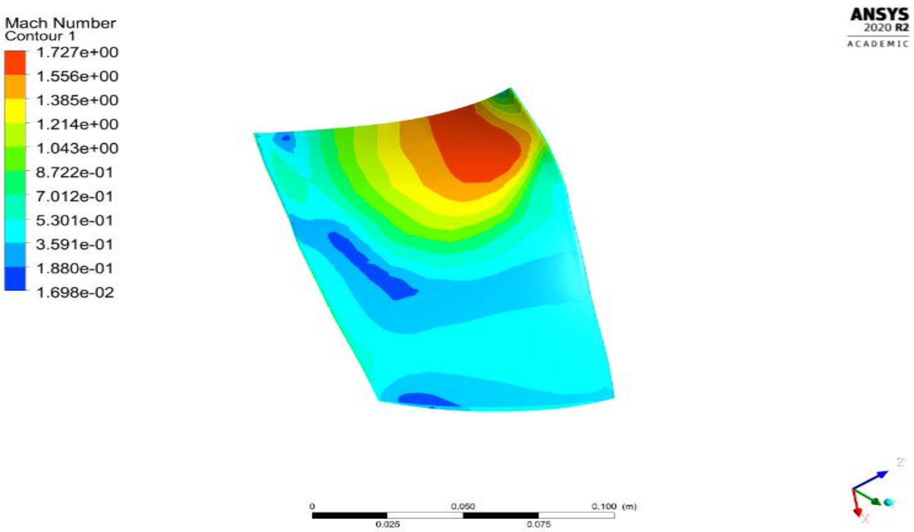

Figure 3 (b) Suction Surface

Fig 3 Mach Number Distribution for Steady State Analysis

The Mach Number and Cp distribution of all the cases for the Grid Independence study is given in Figures 4 and 5 respectively. From this we can conclude that the variation of the mesh sizes does not influence the results at a large rate

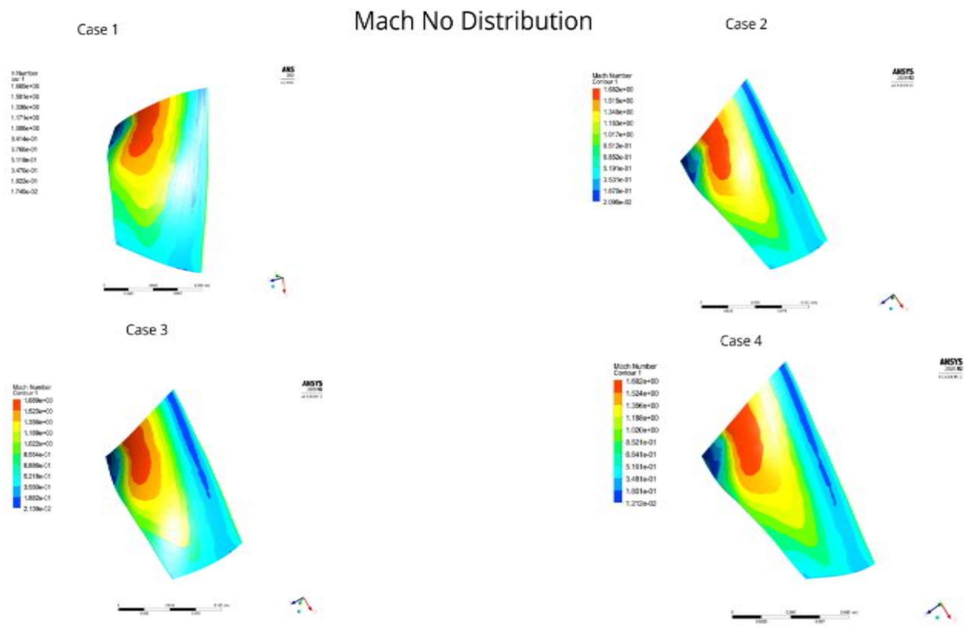

Fig 4 Mach Number Distribution for Grid Independence Study

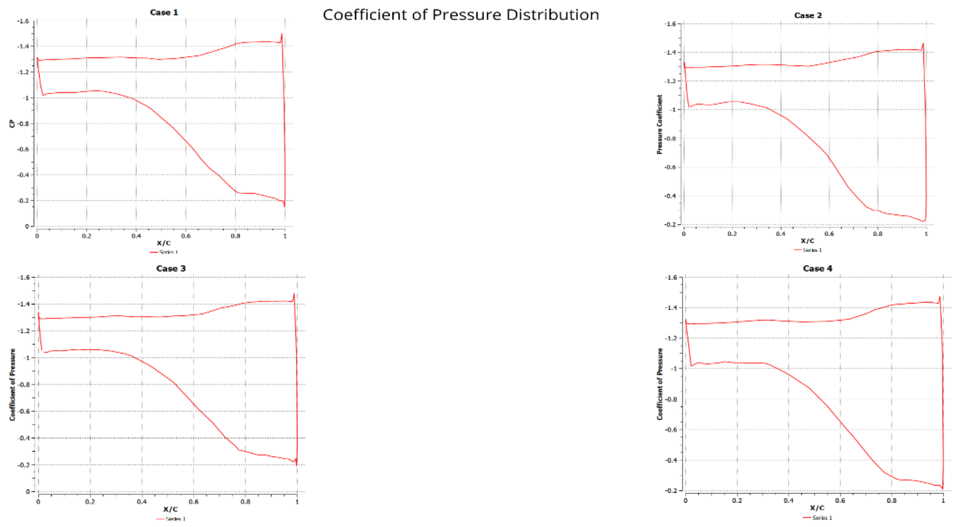

Figure 5 Cp Distribution for Grid Independence Study

3. Off-Design Performance Analysis

For the Off-Design Performance analysis, the speed of the rotor was varied to the speeds given in Table 4. The results obtained at the design speed of 16043 rpm is used as a reference.

Cases	% of Rotational Velocity	Rotational Velocity (rpm)
Case 1	105	16845
Case 2	100	16043
Case 3	96	15041
Case 4	92	14759
Case 5	86	13796

Table 4 – Rotational Speeds for Performance Analysis

The Mach Number Distributions on the Pressure Surface are shown in Figures 6, 7, 8, 9, and 10.

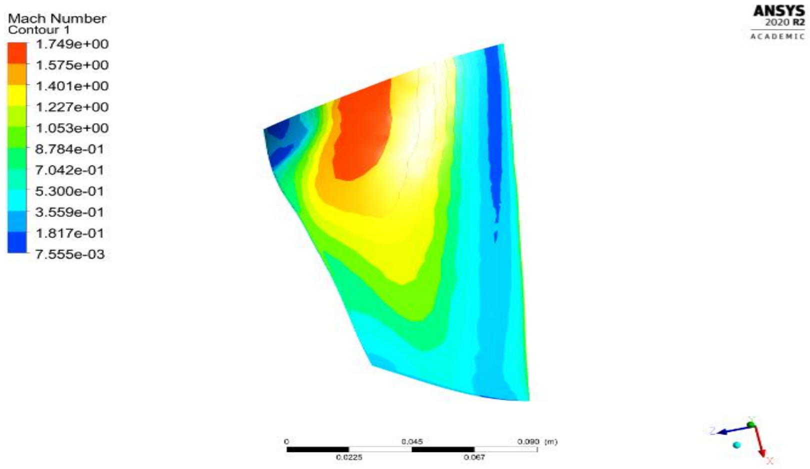

Figure 6 105%

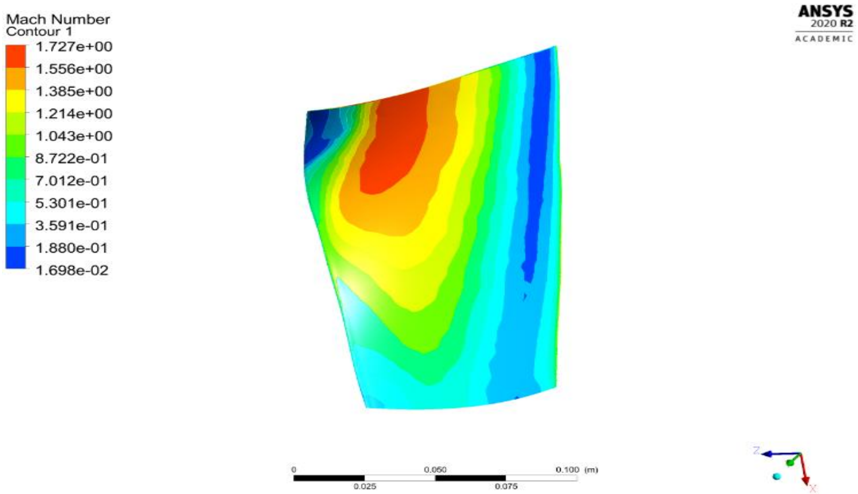

Figure 7 100%

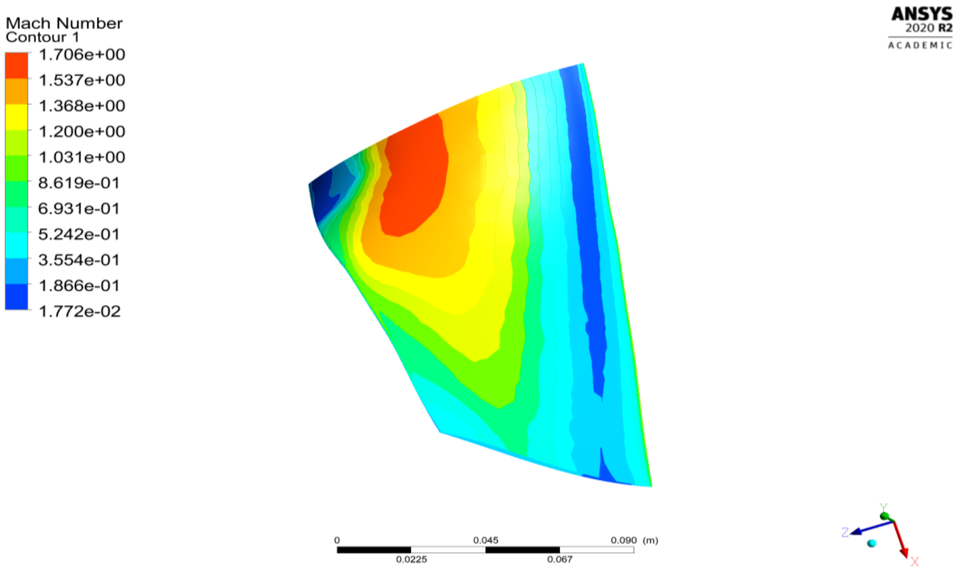

Figure 8 96%

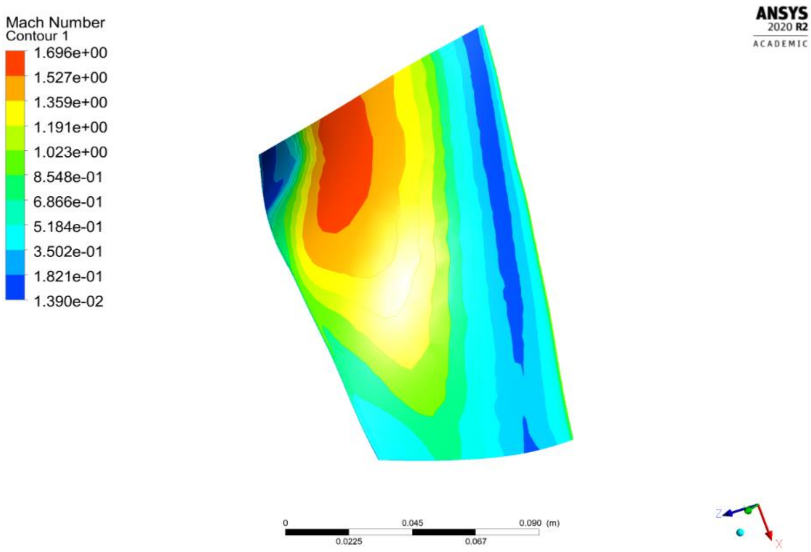

Figure 9 92%

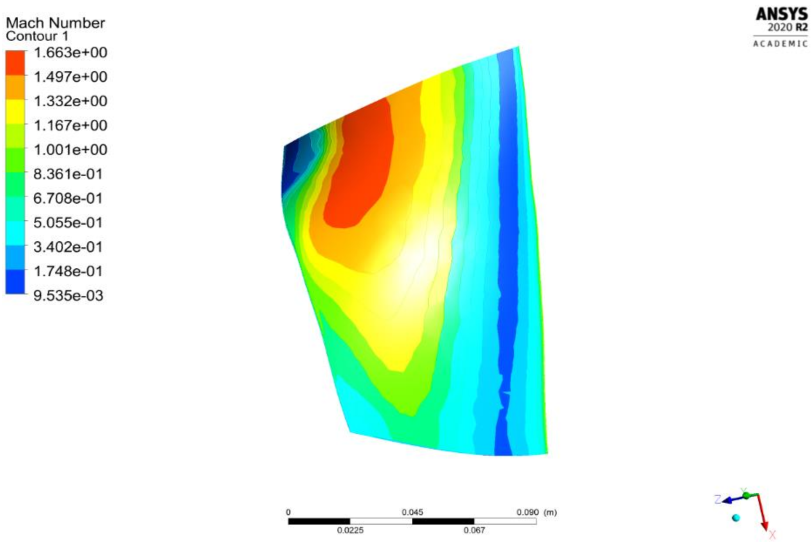

Figure 10 86%

From the above figures, we can see that the location of the shock formed reaches the trailing edge for some speeds. The shock is mainly concentrated around 70% of the span and around 30% of the chord, we can also see that the intensity of the shock decreases as the rotational speed decreases. The variation of pressure ratio across all the five speeds is given in Table 5 and the Cp distribution is given in Fig 11

% of Rotational Velocity	Pressure Ratio
105	1.81
100 (Design Speed)	1.65
96	1.57
92	1.50
86	1.43

Table 5 Variation of Pressure Ratio for Off-design Cases

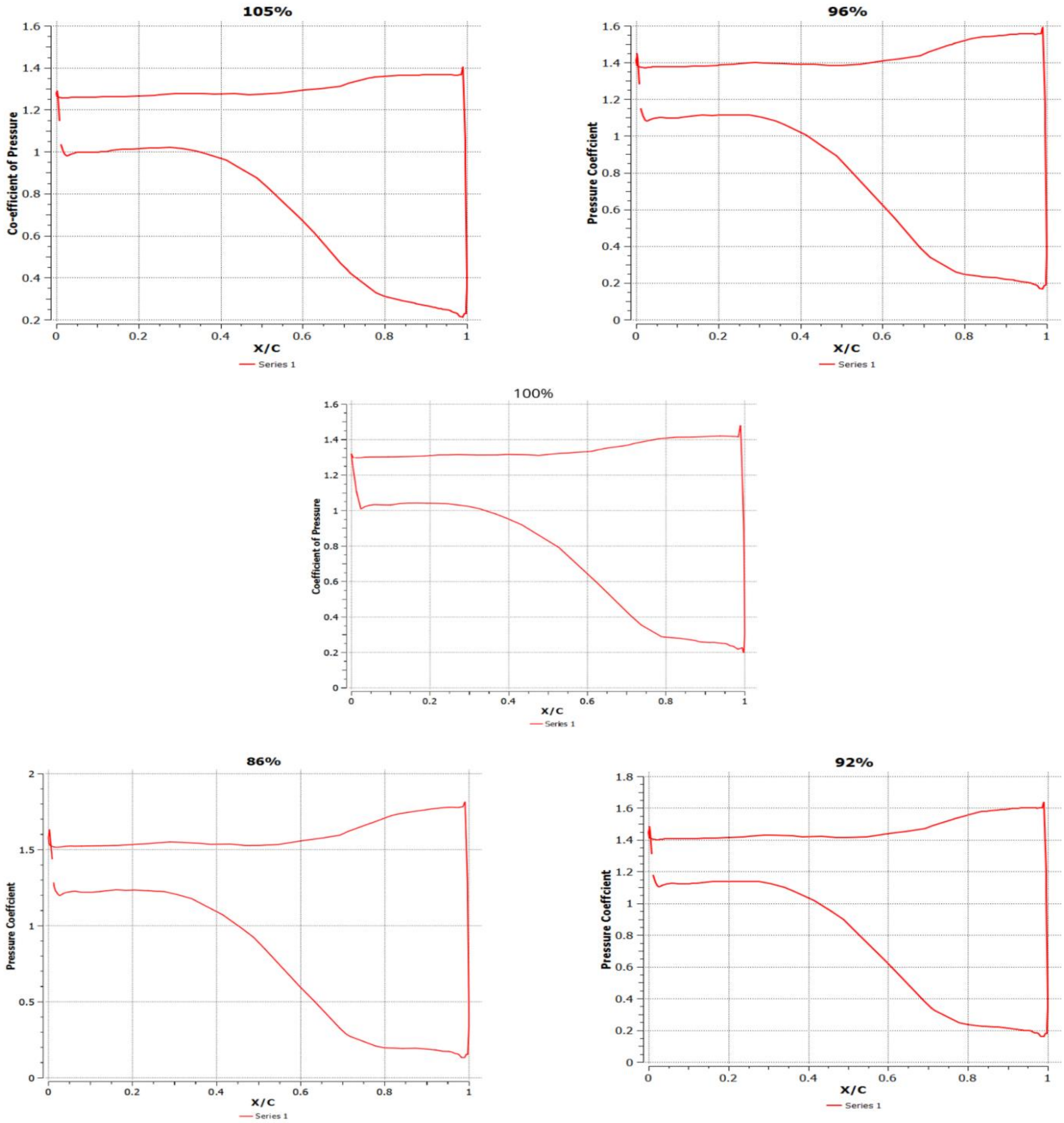

Figure 11 Cp distribution for Off-design Cases

4. Conclusion

From the above Mach Number Contrours, we can conclude the following

- A shock is formed at 70% of the span on the pressure surface and a supersonic bubble is formed near the leading edge of the suction surface
- At various operating conditions, the shock extends from 30% of the chord to the trailing edge and in the span wise direction, it extends from the tip to 30% of the span
- The intensity of the shock formed decreases as the rotational speed is reduced
- The pressure ratio of the rotor also decreases as the rotational speed is reduced.

5. Acknowledgements

The authors would like to thank Dr. Parthasarathy Vasanthakumar for sharing his considerable knowledge on this subject and also for his continued support throughout the project. The authors would also like to thank the Faculty of School of Aeronautical Sciences, Hindustan Institute of Technology and Science for their support.

References

[1] Strazisar A.J., Wood J.R., Hathaway M.D., Suder K.L "Laser Anemometer Measurements in a Transonic Axial-Flow Fan Rotor" NTRS Technical Paper 2879, November 1989

[2] Naseri A., Boroomand M., Sammak S., "Numerical Investigation of Effect of Inlet Swirl and Total-pressure Distortion on Performance and Stability of an Axial Transonic Compressor", Journal of Thermal Sciences Vol 25, No: 6 (2016) 501-510

[3] 7. Patil S., Zori L., Galpin P., Morales J., Godin P "Investigation of Time/Frequency Domain CFD Methods to Predict Turbomachinery Blade Aerodynamic Damping" ASME GT2016-57962 (2016)

[4] ANSYS CFX Documentation

[5] Doi H, Alonso J.J "Fluid Structure Coupled Aeroelastic Computations for Transonic Flows in Turbomachinery" ASME GT-2002-30313